Supplement of The Cryosphere, 18, 1399–1418, 2024
https://doi.org/10.5194/tc-18-1399-2024-supplement

The Cryosphere Open Access EGU

Supplement of

Sea-ice variations and trends during the Common Era in the Atlantic sector of the Arctic Ocean

Ana Lúcia Lindroth Dauner et al.

Correspondence to: Ana Lúcia Lindroth Dauner (ana.lindrothdauner@helsinki.fi, anadauner@gmail.com)

Figures

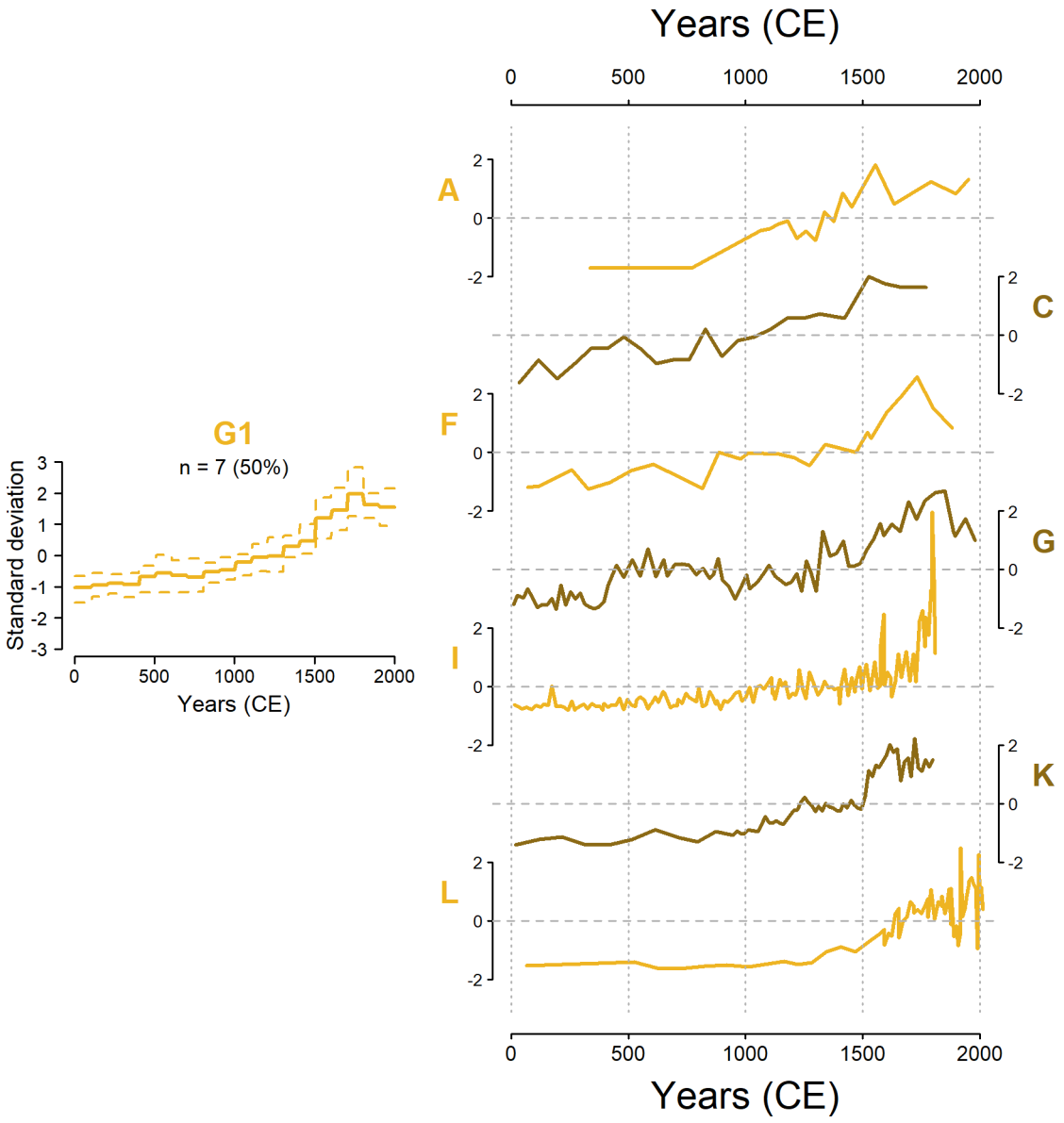

Figure S1. Original data from the records from Group 1 (cluster analysis after removing the global trend).

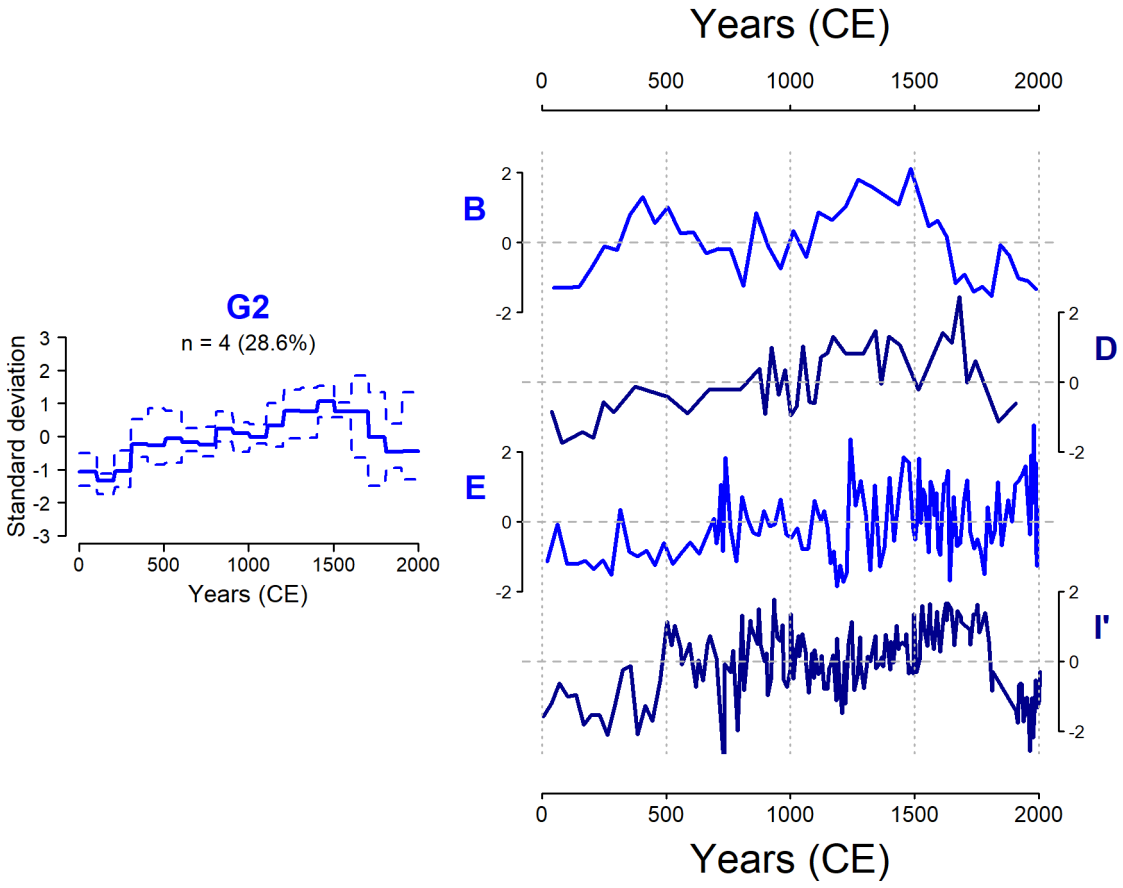

Figure S2. Original data from the records from Group 2 (cluster analysis after removing the global trend).

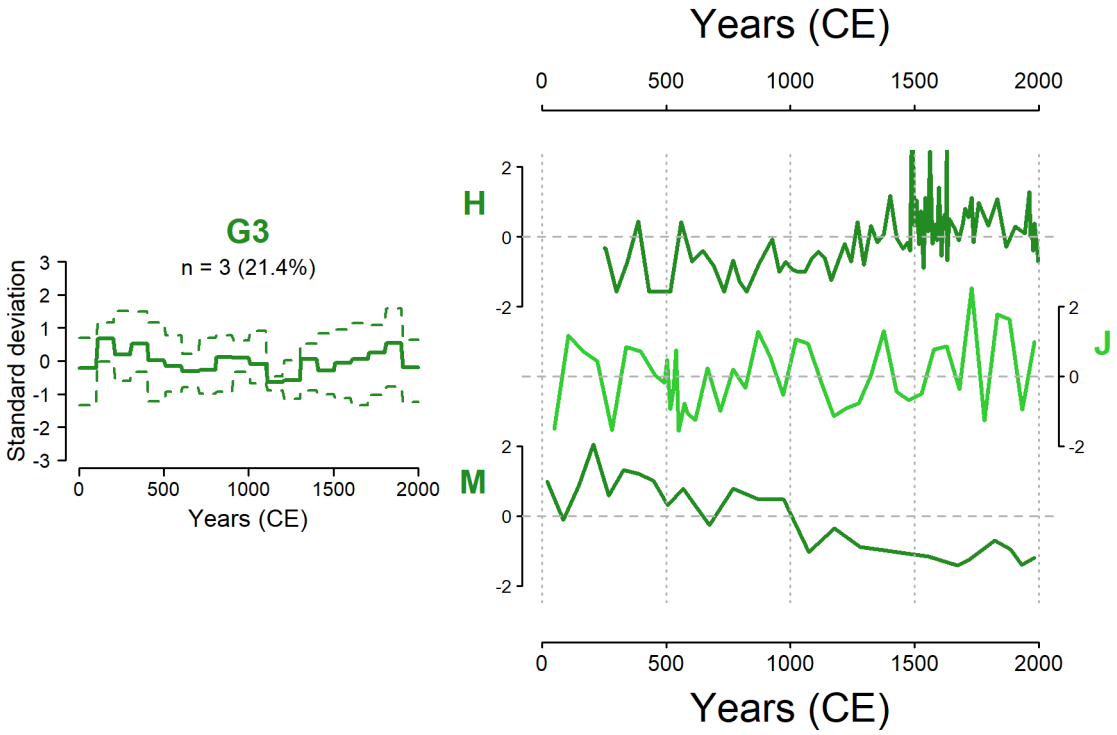

25

Figure S3. Original data from the records from Group 3 (cluster analysis after removing the global trend).

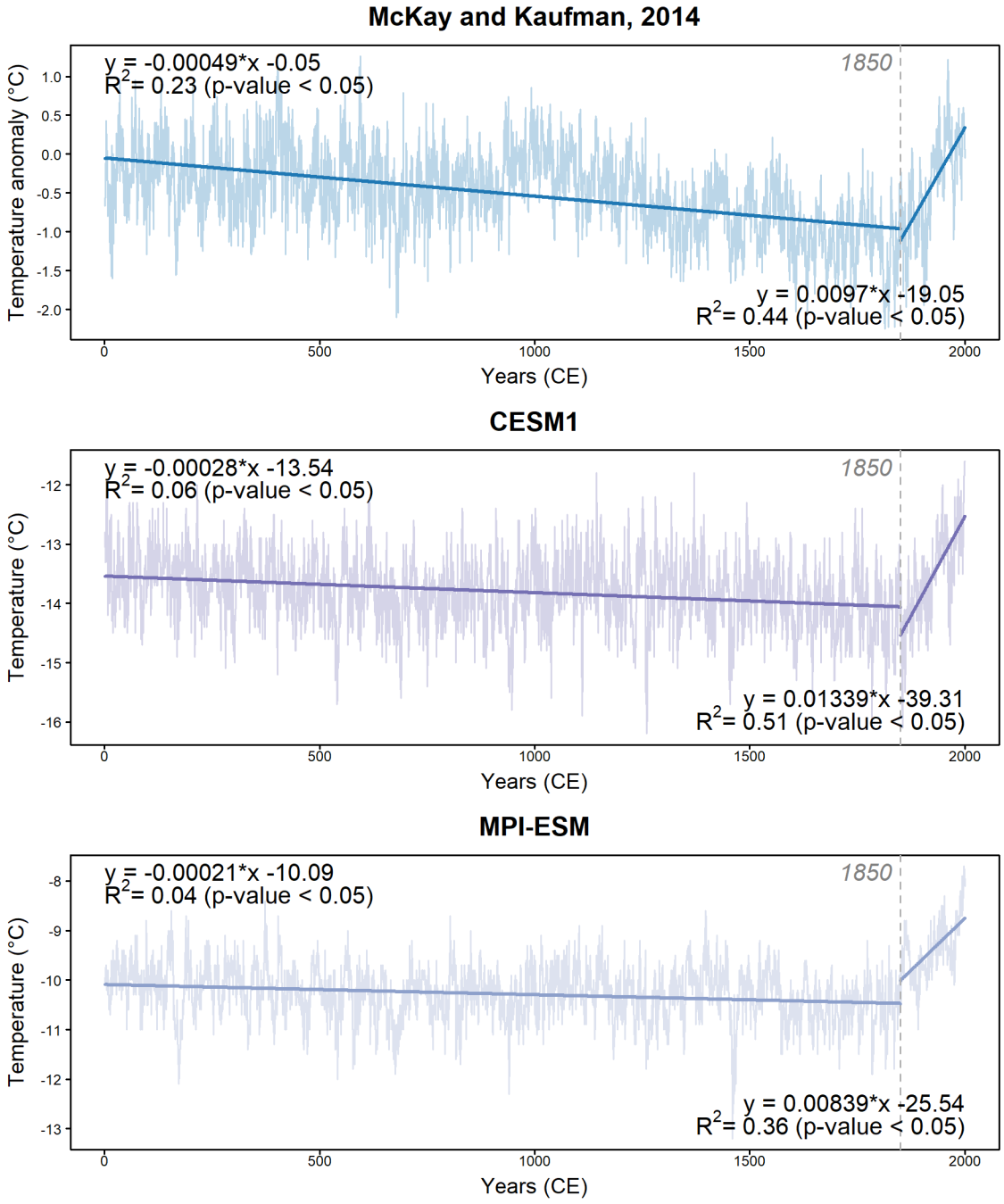

Figure S4. Arctic (latitudes > 60° N) air temperatures based on McKay and Kaufman (2014) and on numerical models CESM1 and MPI-ESM data.

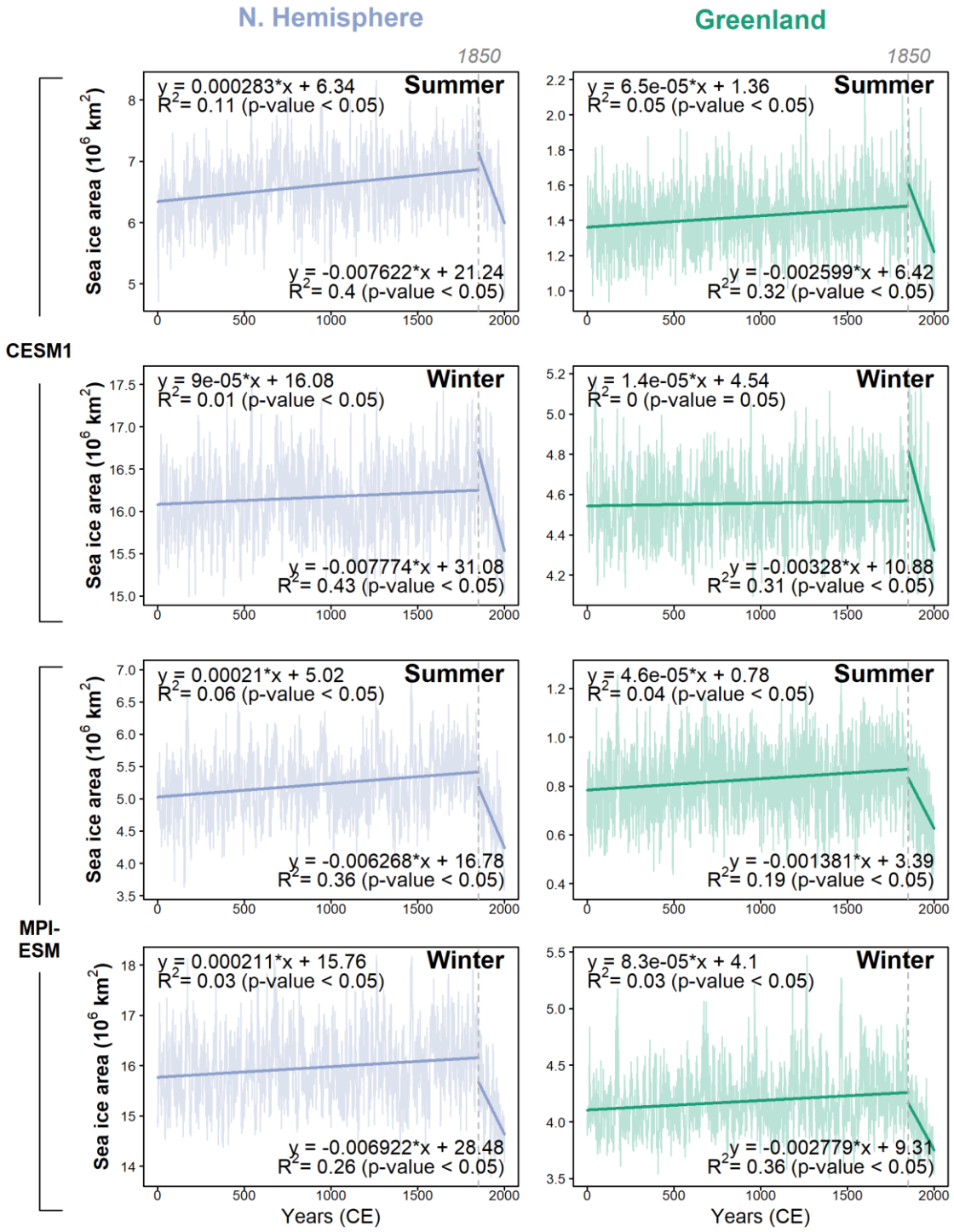

Figure S5. Sea-ice area trends based on numerical models CESM1 and MPI-ESM data, considering the Northern Hemisphere (left column) and region around Greenland (right column), and summer (minimum area) and winter (maximum area) seasons.

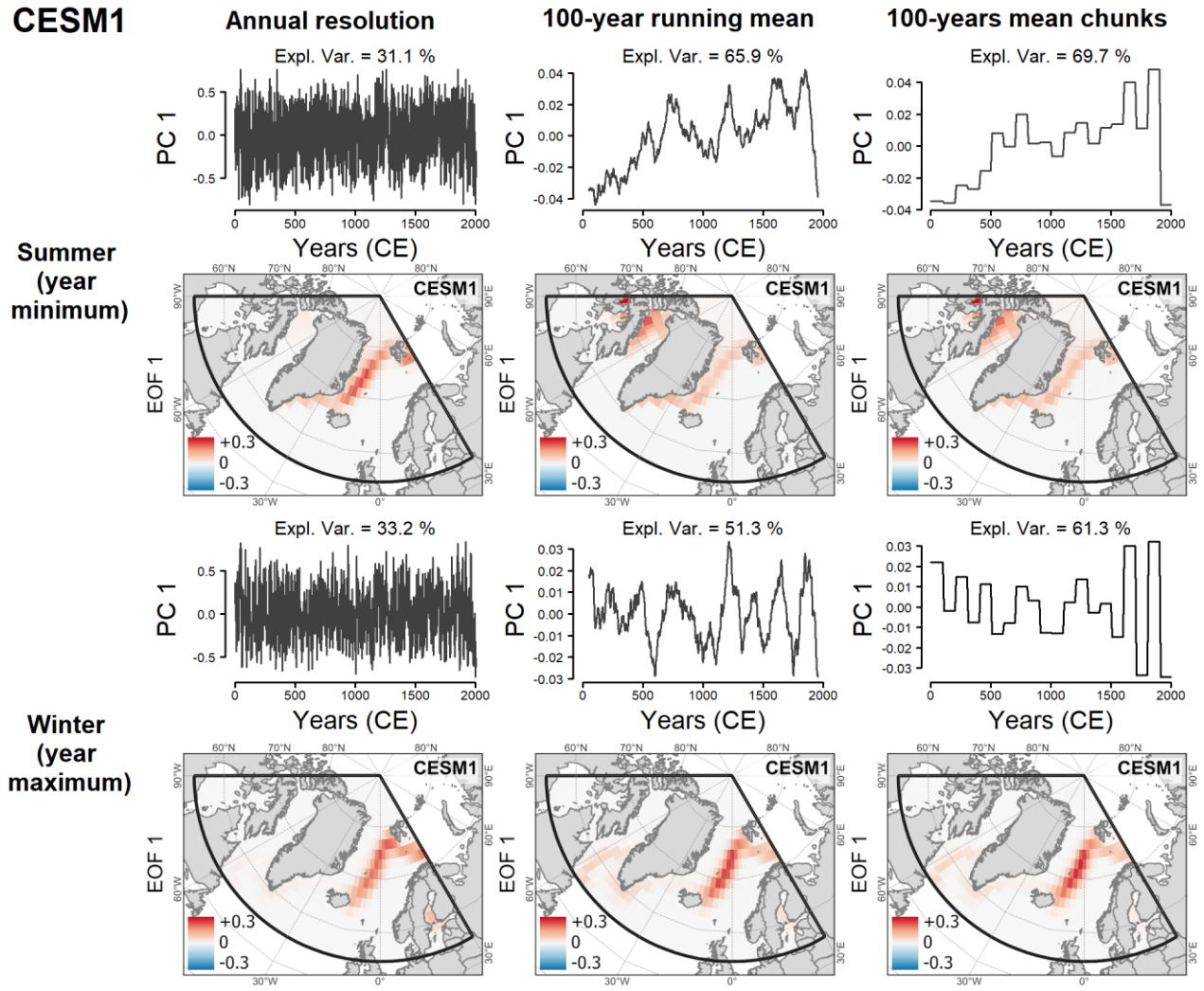

Figure S6. Results of empirical orthogonal function (EOF) analysis (PC1: normalized first principal component; EOF1: first EOF mode loadings) of the sea ice fraction based on CESM1 data, considering summer and winter seasons. First column: Data with annual resolution. Second column: 100-year running mean data. Third column: 100-years mean chunks data. The solid thick black line in the panels of the second and fourth rows represents the spatial domain used in the climate simulations.

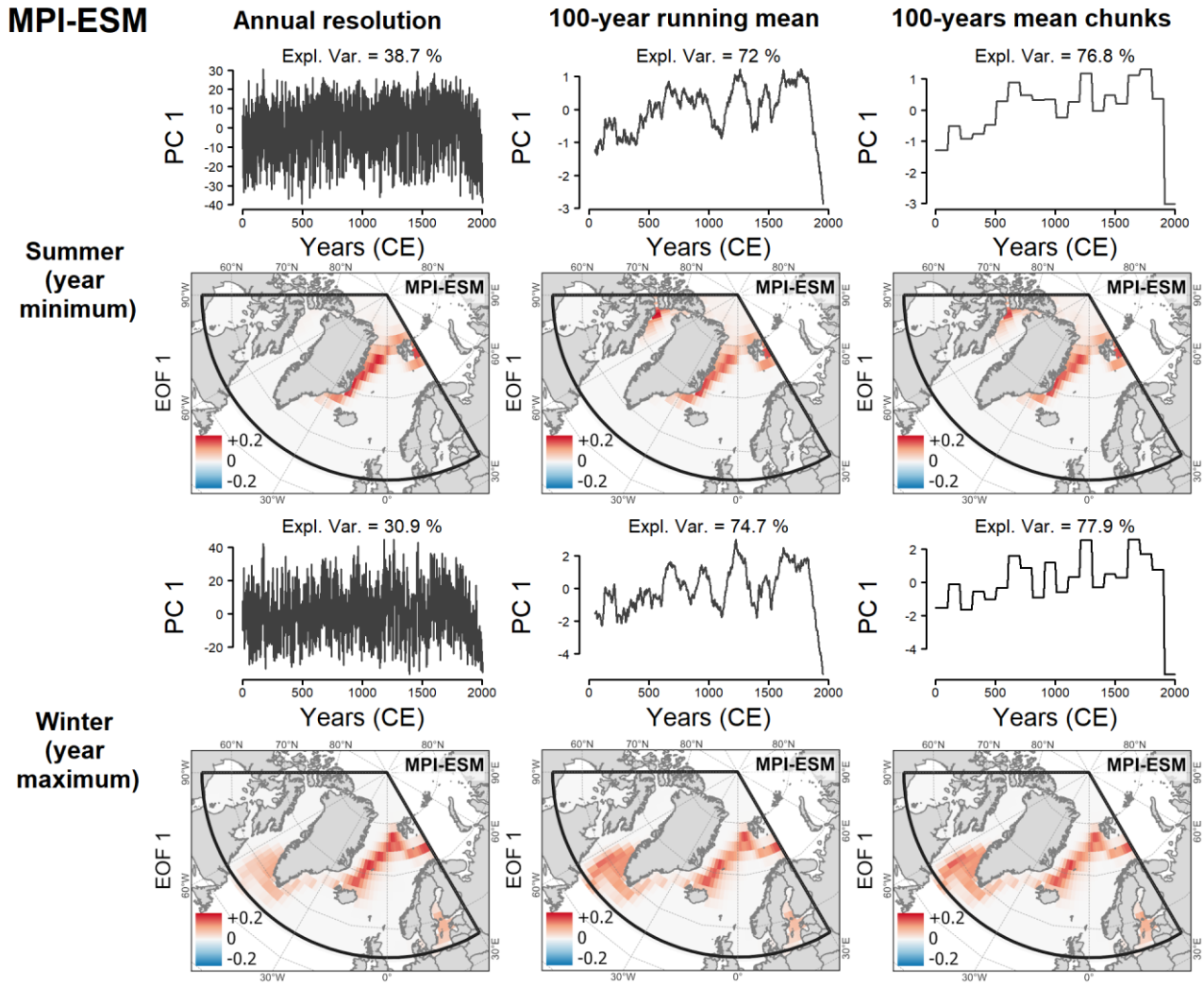

45 **Figure S7. Results of empirical orthogonal function (EOF) analysis (PC1: normalized first principal component; EOF1: first EOF mode loadings) of the sea ice fraction based on MPI-ESM data, considering summer and winter seasons. First column: Data with annual resolution. Second column: 100-year running mean data. Third column: 100-years mean chunks data. The solid thick black line in the panels of the second and fourth rows represents the spatial domain used in the climate simulations.**

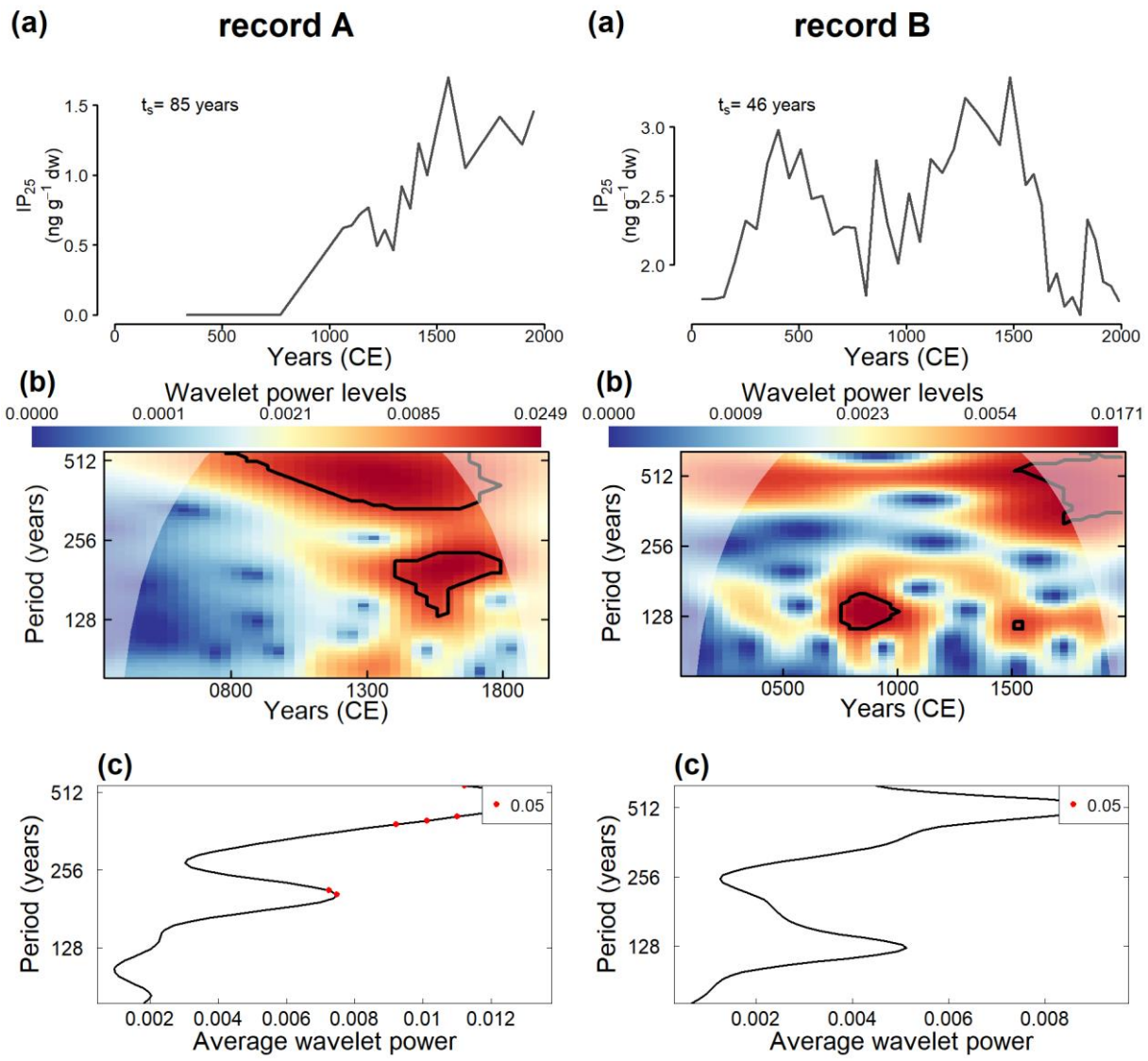

Figure S8. Wavelet analysis of sea ice reconstructions from records A and B. (a) Original time series with the average resolution. (b) Wavelet power spectrum and (c) global wavelet of the normalized signal on the time-frequency domain. Marked regions on the wavelet spectrum indicate significant power to a 95% confidence interval. The areas under the cone of influence show where edge effects are important.

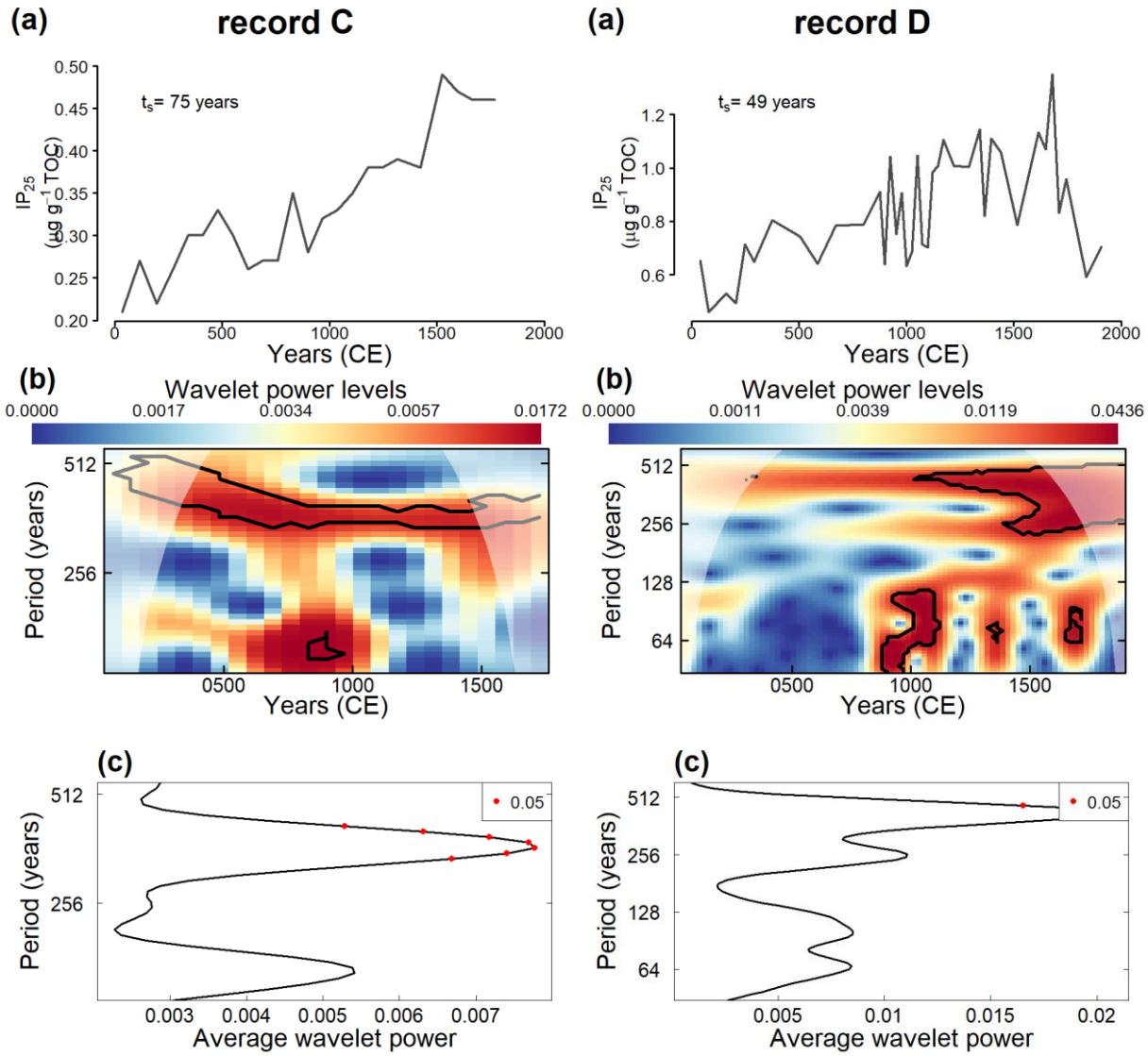

Figure S9. Wavelet analysis of sea ice reconstructions from records C and D. (a) Original time series with the average resolution. (b) Wavelet power spectrum and (c) global wavelet of the normalized signal on the time-frequency domain. Marked regions on the wavelet spectrum indicate significant power to a 95% confidence interval. The areas under the cone of influence show where edge effects are important.

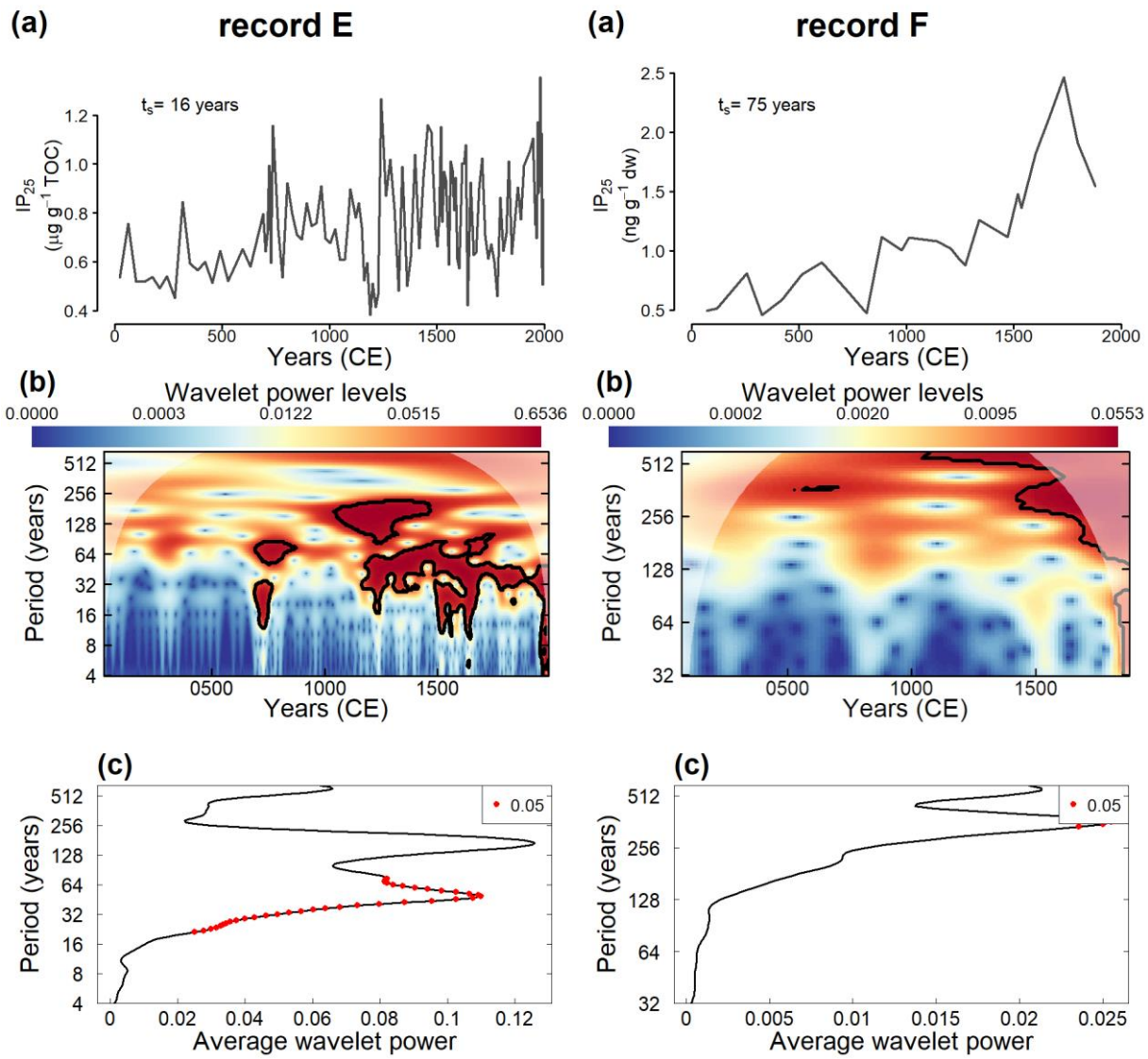

Figure S10. Wavelet analysis of sea ice reconstructions from records E and F. (a) Original time series with the average resolution. (b) Wavelet power spectrum and (c) global wavelet of the normalized signal on the time-frequency domain. Marked regions on the wavelet spectrum indicate significant power to a 95% confidence interval. The areas under the cone of influence show where edge effects are important.

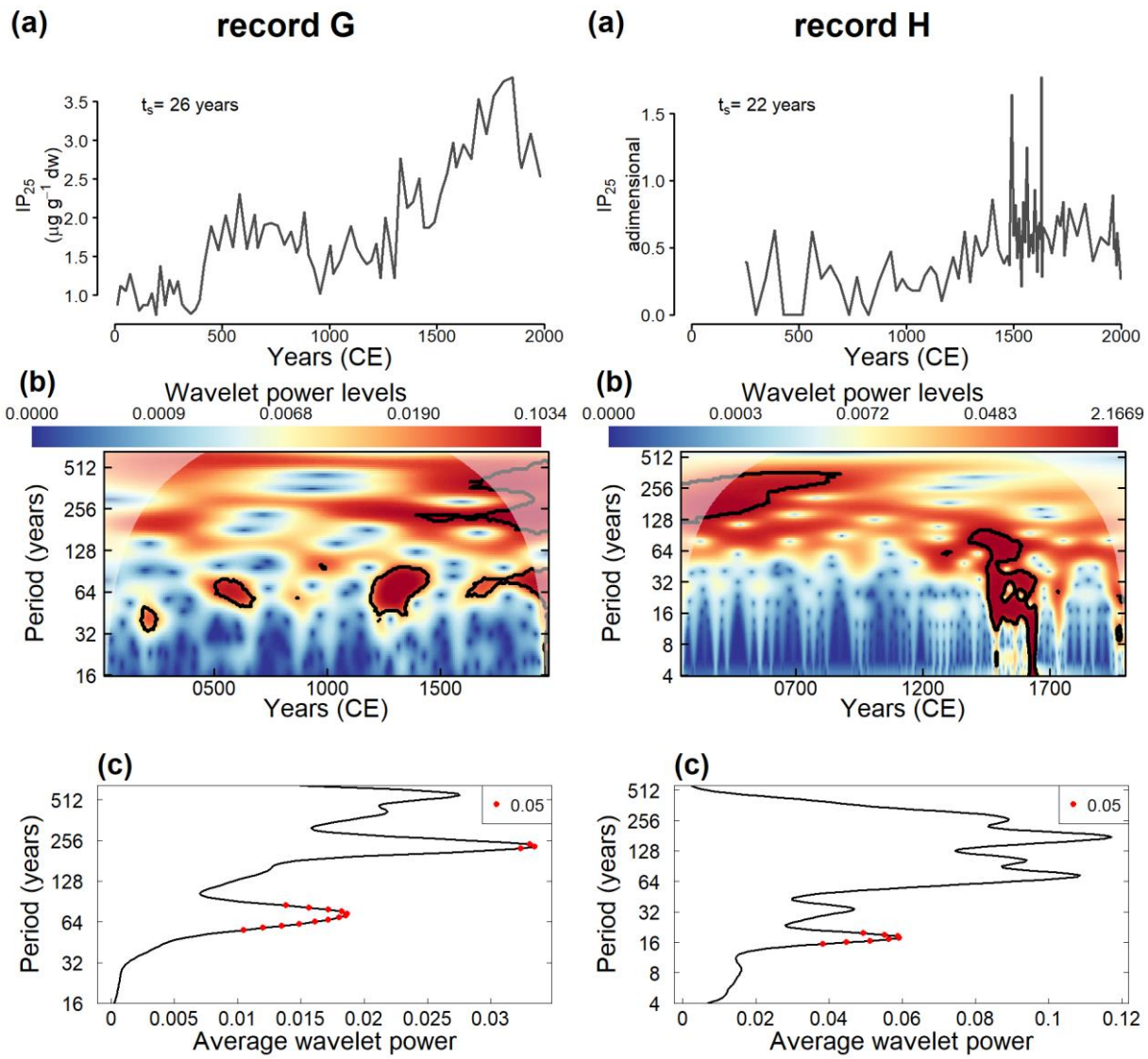

Figure S11. Wavelet analysis of sea ice reconstructions from records G and H. (a) Original time series with the average resolution. (b) Wavelet power spectrum and (c) global wavelet of the normalized signal on the time-frequency domain. Marked regions on the wavelet spectrum indicate significant power to a 95% confidence interval. The areas under the cone of influence show where edge effects are important.

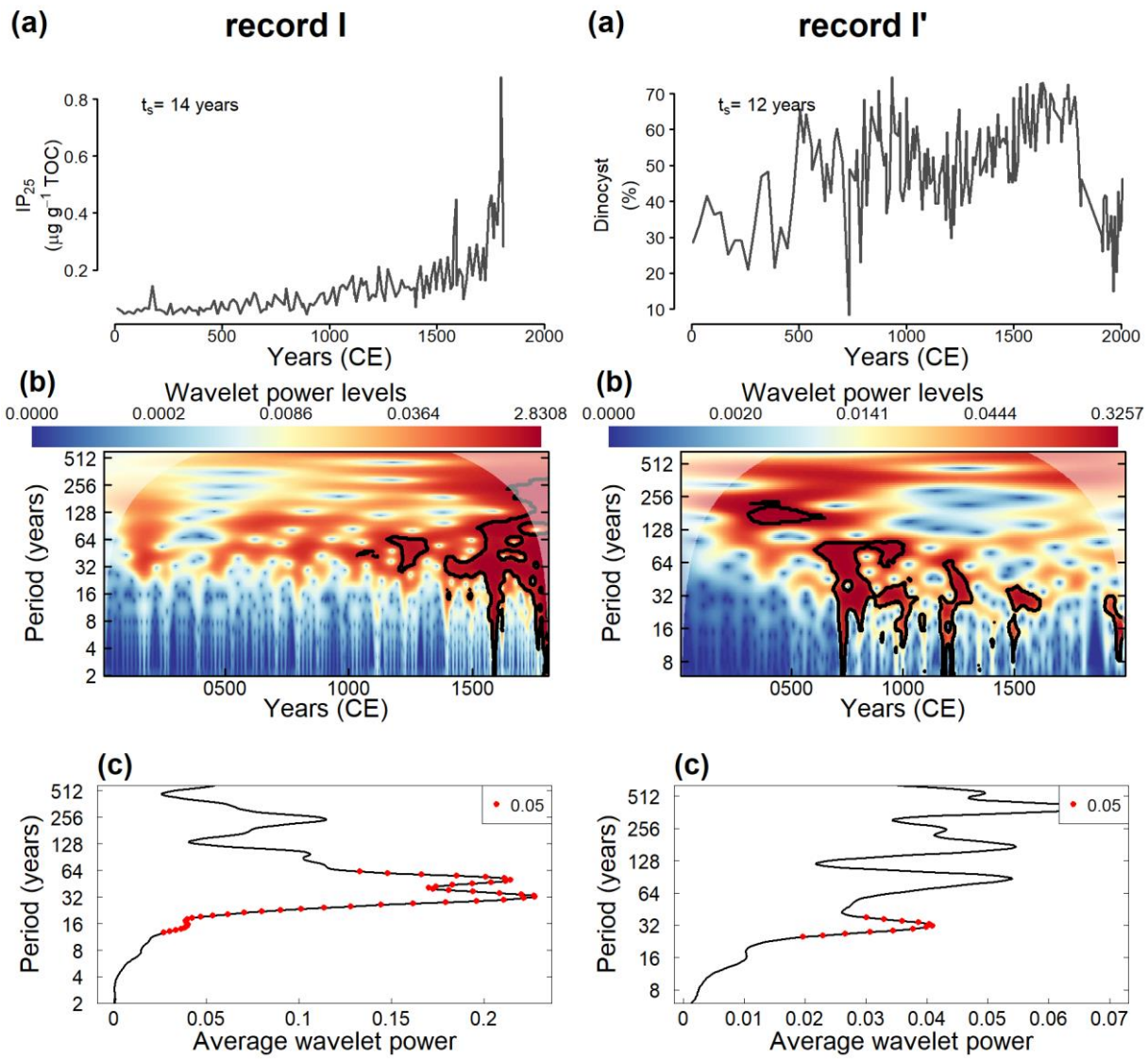

Figure S12. Wavelet analysis of sea ice reconstructions from records I and I'. (a) Original time series with the average resolution. (b) Wavelet power spectrum and (c) global wavelet of the normalized signal on the time-frequency domain. Marked regions on the wavelet spectrum indicate significant power to a 95% confidence interval. The areas under the cone of influence show where edge effects are important.

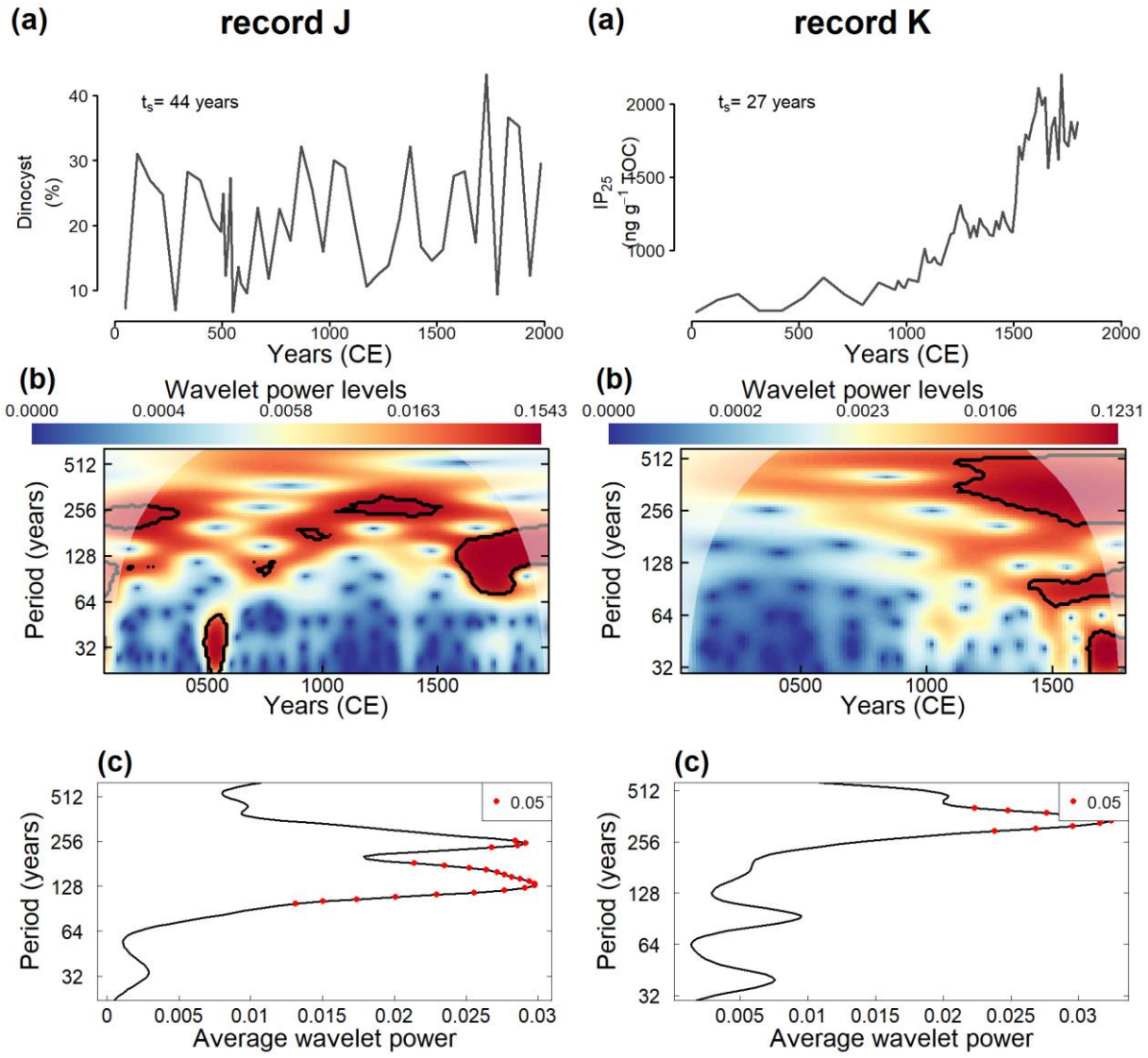

Figure S13. Wavelet analysis of sea ice reconstructions from records J and K. (a) Original time series with the average resolution. (b) Wavelet power spectrum and (c) global wavelet of the normalized signal on the time-frequency domain. Marked regions on the wavelet spectrum indicate significant power to a 95% confidence interval. The areas under the cone of influence show where edge effects are important.

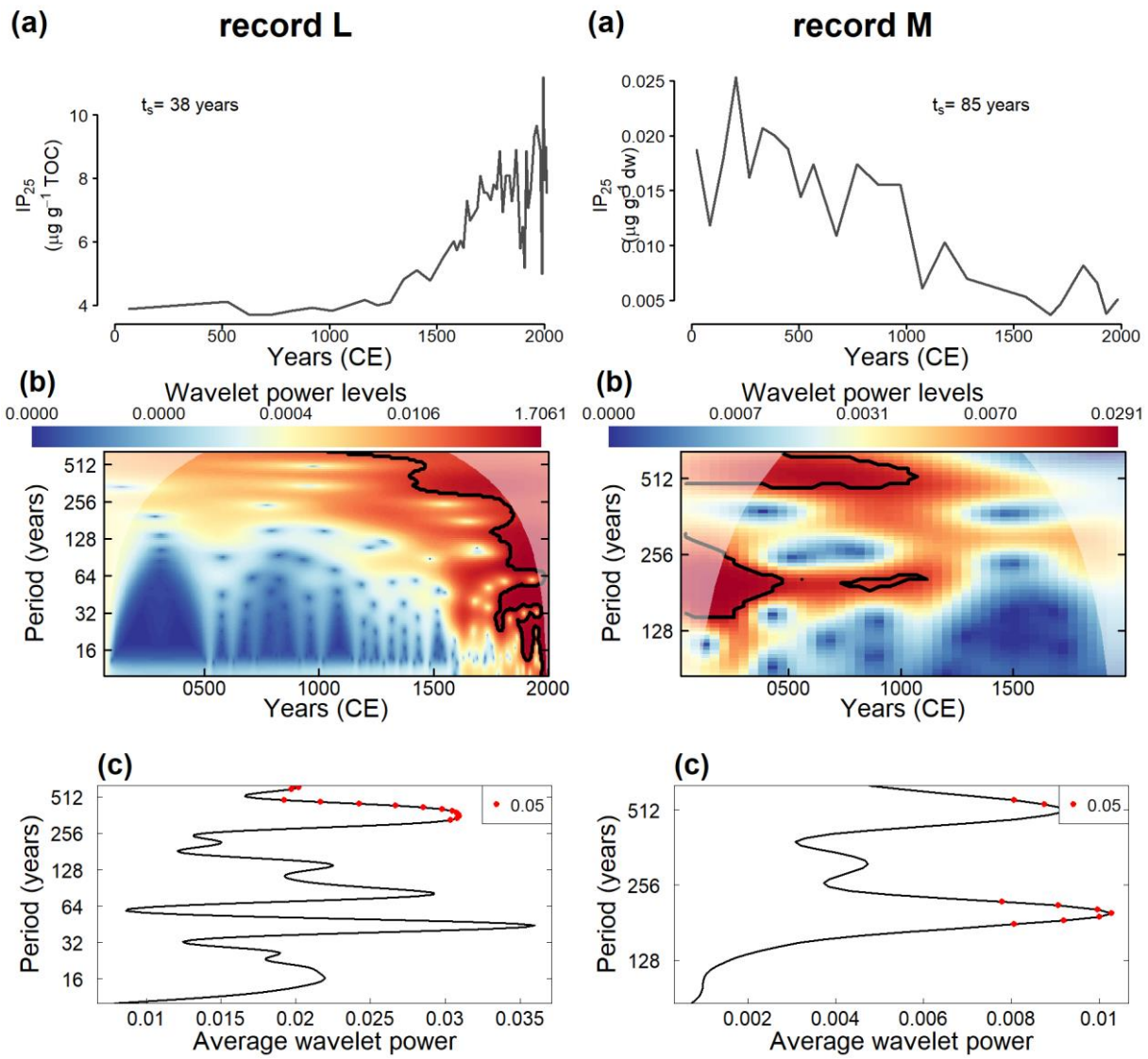

Figure S14. Wavelet analysis of sea ice reconstructions from records L and M. (a) Original time series with the average resolution. (b) Wavelet power spectrum and (c) global wavelet of the normalized signal on the time-frequency domain. Marked regions on the wavelet spectrum indicate significant power to a 95% confidence interval. The areas under the cone of influence show where edge effects are important.

Tables

Table S1. Values of the average composite of the standardized sea-ice reconstructions used in this study, considering the mean values after binning to 100-year time slices.

Time slice	All records (n = 14)	G1 (n = 7)	G2 (n = 4)	G3 (n = 3)
0 - 100	-0.816	-1.031	-1.060	-0.219
100 - 200	-0.659	-0.945	-1.343	0.688
200 - 300	-0.724	-0.889	-1.056	0.203
300 - 400	-0.483	-0.921	-0.224	0.527
400 - 500	-0.514	-0.684	-0.274	0.015
500 - 600	-0.394	-0.560	-0.067	-0.161
600 - 700	-0.461	-0.648	-0.175	-0.312
700 - 800	-0.478	-0.697	-0.246	-0.279
800 - 900	-0.168	-0.523	0.236	0.126
900 - 1000	-0.164	-0.468	0.088	0.106
1000 - 1100	-0.138	-0.217	-0.021	-0.088
1100 - 1200	-0.133	-0.066	0.330	-0.632
1200 - 1300	-0.017	-0.016	0.767	-0.591
1300 - 1400	0.281	0.282	0.751	0.049
1400 - 1500	0.395	0.467	1.064	-0.292
1500 - 1600	0.813	1.206	0.762	-0.050
1600 - 1700	1.086	1.462	0.758	0.068
1700 - 1800	1.240	1.987	-0.017	0.255
1800 - 1900	1.281	1.628	-0.475	0.537
1900 - 2000	1.134	1.557	-0.444	-0.188

Table S2. Comparison between simulated sea-ice areas (in million km^2) between the two models (CESM1 and MPI-ESM) and sea-ice extent (in million km^2) from satellite data (obtained from the Integrated Climate Data Center, University of Hamburg - https://www.fdr.uni-hamburg.de/record/8559) for the Northern Hemisphere for annual, summer and winter areas, over the period between 1979 – 2000 CE. For the complete names of the sea-ice areas, please check Doerr et al. (2021).

Sea-ice area (10^6 km^2) between 1979-2000		**Northern Hemisphere**		
		Minimum area	Annual average area	Maximum area
CESM1	Summer	4.8	6.0	6.6
	Winter	15.0	15.6	16.2
MPI-ESM	Summer	3.6	4.2	4.8
	Winter	14.1	14.6	15.1
HadISST_orig	Summer	5.8	6.7	7.5
	Winter	15.3	15.7	16.3
HadISST_nsidc	Summer	5.8	6.7	7.4
	Winter	14.8	15.3	15.8
nsidc_bt	Summer	5.6	6.5	7.3
	Winter	14.4	14.9	15.5
nsidc_nt	Summer	4.6	5.3	6.0
	Winter	13.4	14.0	14.5
osisaf	Summer	5.0	5.7	6.3
	Winter	13.7	14.2	14.7
walsh	Summer	5.5	6.4	7.2
	Winter	14.7	15.3	16.0

Doerr, J., Notz, D., and Kern, S.: UHH Sea Ice Area Product (Version 2019_fv0.01) [Data set], https://doi.org/http://doi.org/10.25592/uhhfdm.8559, 2021.